Computational and Structural Biotechnology Journal 21 (2023) 1851–1859

Contents lists available at ScienceDirect

Computational and Structural Biotechnology Journal

journal homepage: www.elsevier.com/locate/csbj

Research article

Automated pancreatic islet viability assessment for transplantation using bright-field deep morphological signature

Abbas Habibalahi [a,b,*,1], Jared M. Campbell [a,b,2], Stacey N. Walters [c,d,e,3], Saabah B. Mahbub [a,b,4], Ayad G. Anwer [a,b,5], Shane T. Grey [c,d,e,**,6,7], Ewa M. Goldys [a,6,8]

[a] Graduate School of Biomedical Engineering, University of New South Wales, Sydney, NSW 2052, Australia
[b] Australian Research Council Centre of Excellence for Nanoscale BioPhotonics, Australia
[c] Garvan Institute of Medical Research, Darlinghurst, New South Wales, Australia
[d] Faculty of Medicine, University of New South Wales, Sydney, NSW, Australia
[e] St Vincent's Clinical School, The University of New South Wales, Sydney, NSW, 2010 Australia

ARTICLE INFO

Article history:
Received 22 November 2022
Received in revised form 20 February 2023
Accepted 22 February 2023
Available online 24 February 2023

Keywords:
Pancreatic islet
Transplantation
Deep morphological signature

ABSTRACT

Islets transplanted for type-1 diabetes have their viability reduced by warm ischemia, dimethyloxalylglycine (DMOG; hypoxia model), oxidative stress and cytokine injury. This results in frequent transplant failures and the major burden of patients having to undergo multiple rounds of treatment for insulin independence. Presently there is no reliable measure to assess islet preparation viability prior to clinical transplantation. We investigated deep morphological signatures (DMS) for detecting the exposure of islets to viability compromising insults from brightfield images. Accuracies ranged from 98 % to 68 % for; ROS damage, pro-inflammatory cytokines, warm ischemia and DMOG. When islets were disaggregated to single cells to enable higher throughput data collection, good accuracy was still obtained (83–71 %). Encapsulation of islets reduced accuracy for cytokine exposure, but it was still high (78 %). Unsupervised modelling of the DMS for islet preparations transplanted into a syngeneic mouse model was able to predict whether or not they would restore glucose control with 100 % accuracy. Our strategy for constructing DMS' is effective for the assessment of islet pre-transplant viability. If translated into the clinic, standard equipment could be used to prospectively identify non-functional islet preparations unable to contribute to the restoration of glucose control and reduce the burden of unsuccessful treatments.

1. Introduction

In type-1 diabetes the destruction of insulin secreting beta-cells in pancreatic islets results in elevated blood glucose levels. This results in the multiple morbidities, including heart, kidney, nerve and eye damage, leading to reduced quality of life and earlier mortality. Allogenic transplant of pancreatic islets can restore glucose control, however its efficiency as a therapy is low, with most patients requiring repeated transplants with high islet numbers to achieve insulin independence [1,2]. Islet viability is frequently compromised by pathological "insults" experienced by islets donated for transplantation. Examples of these include warm ischemia, hypoxia, oxidative stress and cytokine injury. The failure of transplantation often occurs due to this compromised viability [2]. As such, an assay for characterising islet preparations to inform clinical decision making prior to transfer as to whether a procedure has sufficient likelihood of success to be worth proceeding with, has long been identified as an area of need [3].

Abbreviations: AI, artificial intelligence; DMOG, dimethyloxalylglycine; DMS, deep morphological signatures; ECG, electrocardiogram; EEG, electroencephalogram; EMCCD, electron multiplying charge coupling device; FD, Fisher Distance; GSIS, glucose stimulated insulin secretion; IoU, intersection over union; MRI, magnetic resonance imaging; MEG, magnetoencephalography; ROS, reactive oxygen species; SI, swarm intelligence; SVM, support vector machine; PCA, principal component analysis

* Corresponding author at: Graduate School of Biomedical Engineering, University of New South Wales, Sydney, NSW 2052, Australia.
** Corresponding author at: Garvan Institute of Medical Research, Darlinghurst, NSW, Australia.
E-mail addresses: a.habibalahi@unsw.edu.au (A. Habibalahi), s.grey@garvan.org.au (S.T. Grey).
[1] ORCID 0000-0001-7833-1705
[2] ORCID 0000-0003-0163-4251
[3] ORCID 0000-0001-5937-2341
[4] ORCID 0000-0002-3320-2499
[5] ORCID 0000-0002-2029-1023
[6] These authors share co-senior authorship
[7] ORCID 0000-0003-2160-1625
[8] ORCID 0000-0003-2470-7118

https://doi.org/10.1016/j.csbj.2023.02.039

Methodologies for estimating islet viability have been developed; including observer assessment of islet morphology, exposure to membrane impermeable fluorescent dyes for the detection of dead cells), comparison of the ATP/ADP ratio and measurement glucose stimulated insulin secretion (GSIS). However, none of these are strongly predictive of insulin independence after transplant [3–8]. This has been hypothesised to be due to pre-transplantation assessment of live/dead cells not apoptotic and pre apoptotic cells, as well as recovery of insulin secretion by quiescent beta-cells upon reintroduction to the physiological environment [3].

We recently demonstrated successful restoration of glucose control in diabetic mice could be predicted from the hyperspectral assessment of islet autofluorescence [9]. Cellular morphology is known to be strongly influenced by the cell's microenvironment and responsive to biophysical and environmental factors [10]. As such, we have extended this program to use deep learning technology to discover specific morphological cell signatures, reflective of cell viability and quality, but hitherto imperceptible to human assessment from simple brightfield images. This would have the translational advantage of enabling islet assessment without specialist equipment. A bottleneck in studying cell morphology has been the development of suitable automatic processing tools to extract the huge amount of information that is available in cell images. In recent years, however, there has been increasing interest in the application of artificial intelligence (AI) to biomedical image assessment for diagnosis, quality assessment and disease monitoring. AI has enhanced precise treatment customization plans [11] and unlocked new information in medical images which was previously overlooked due to natural human limitations in extracting comprehensive image features. In particular, deep learning techniques have been applied to interpret electrocardiogram (ECG), electroencephalogram (EEG), magnetic resonance imaging (MRI) and magnetoencephalography (MEG) where it showed excellent improvements in reliability and precision decision making [12].

In this study, we defined a deep morphological signature (DMS) based on a novel combination of advanced AI methods including deep learning, and swarm intelligence followed by discriminative analysis applied to brightfield microscopy images of whole and disaggregated islets for their quality assessment. DMS, an automated, quantitative approach for extracting information, was applied to segmented images of islets to extract morphological information using deep structured nets that capture features such as shapes and textures. This approach is sensitive to image differences at perceptible and imperceptible levels. The other elements of our analytic strategy enable the development of accurate models from relatively limited sample sizes (deep learning approaches normally require many thousands of samples to adequately train) and has previously been successfully applied to the assessment of oocyte quality where it was able to accurately detect advanced maternal age and was sensitive to the mitigatory effects of a geroprotective intervention [13]. Bright-field microscopy was used in this study as it is the simplest of all the optical microscopy illumination techniques, requires only basic equipment, and therefore has high translatability.

Our aim was to develop DMS' able to accurately detect the exposure of islets to viability compromising insults, including reactive oxygen species (ROS), dimethyloxalylglycine (DMOG; a hypoxia mimetic that stabilises hypoxia inducible factor as a model of exposure to a low oxygen environment), pro-inflammatory cytokines and warm ischemia (modelling potential delays in the clinical collection of organs from consenting donors) from brightfield images of islets. Furthermore, although imaging whole islets hypothetically provides inherent information on their viability through their structure and composition, we also investigated the application of this methodology to single cells from disaggregated islets as it is a far higher throughput approach which is still representative of the full sample. We also investigated whether a DMS could still be developed if islets were encapsulated in a conformal coating as is being investigated for the avoidance of immune detection. Finally, we investigated whether our demonstrated sensitivity to exposure to viability compromising insults would enable prediction of whether islet preparations would be successful or unsuccessful at restoring glucose control in diabetic mice. The use of unsupervised assessment here was important as by not "instructing" the algorithm to differentiate viable from non-viable preparations, and instead allowing it to sort like with like according to emergent differences, we obviated the issue of model overfitting.

2. Methods

Brightfield images used in this study were taken alongside hyperspectral images whose assessment was previously reported in Campbell et al. 2022 [9]. Ethics approval was from the Garvan Institute of Medical Research Animal Research Authority (20_18).

2.1. Islet collection and culture

Pancreatic islets were collected from mice (2–3 C57BL/6Ausb mice (Australian BioResources) per experiment (mixed sex)) and cultured as described in [9]. In brief, exposures were 2 h 30 μM menadione (ROS clearance inhibition) followed by 24 h normal culture, 16 h 0.5 mM/L DMOG followed by immediate imaging, 24 h 200 U/μL TNF-α, 200 U/μL IFNγ, and 25 U/μL IL-1β (pro-inflammatory signalling) followed by immediate imaging, or 60 min delayed collection of pancreases (warm ischaemia) followed by 24 h culture. In all cases, control islets were maintained in culture media for an identical time-courses. Islets from different mice were pooled for the ROS, DMOG and inflammatory models prior to being sorted into the different treatment groups. This ensured that differences were not a consequence of animal or extraction specific factors. In the warm ischemia experiment the intervention had to be carried out at the animal level. As such three mice were used for the control and intervention groups. For single cell assessment islets were disaggregated in 0.5 mM EDTA. For the encapsulation experiment a hydrogen-bonded (PVPON/TA)n multilayer film was applied as described in [9]. Disaggregation of islets was performed with 0.5 mM EDTA.

2.1.1. Islet transplantation

Transplant recipients were 8–10 week old C57BL/6Ausb mice who had diabetes induced by intravenous injection of 20 mg/ml alloxan tetrahydrate (Sigma-Aldrich) per 110 mg/kg body weight. A blood glucose of ≥ 20 mmol/l on consecutive readings was required to be eligible to be a transplant recipient. Islets were isolated from pooled pancreata of three donor mice (to ensure adequate numbers per preparation) and transplanted into syngenic recipients [14]. One hundred islets (hand counted) were transplanted into recipient mice. Islets were either isolated immediately (control) or exposed to 60 min of warm ischemia. The transplantation surgical procedure was performed as described in [9]. Post-transplant follow up was carried out for 30 days. Islet preparations were defined as restoring blood glucose control is mice had blood glucose at ≤20 mmol/l at the end of this period.

2.2. Image collection and data analysis

Brightfield microscopy was performed using an Olympus IX83 microscope with a NuVu electron multiplying charge coupling device camera (EMCCD, hnu1024). To define the DMS we combined deep learning, swarm intelligence and discriminative analysis as shown in Fig. 1. First, brightfield images of islets or cells were segmented to define regions of interest. Images were augmented to artificially expand the dataset through the addition of versions

intuitively equivalent to the originals [15]. Cell images were then provided to deep learning nets constructed to extract deep features. Further, the data set were cross validated to training (80 %) to discover DMS and testing (20 %) subsets for later DMS validation [16]. Through iterative application of swarm intelligence (SI) and discriminative analysis, DMS is discovered incorporating a predefined number of deep learning features [17]. In a loop, SI proposed features candidate and discriminative analysis defines the DMS by representing data points in a 2-D discriminative space spanned by the two canonical variables [18]. These canonical variables were optimal linear combinations of selected features and provides the highest separation of data clusters as measured by the Fisher Distance (FD) [19–21]. FD is the criterion function of the DMS strength and is evaluated in each iteration. Iteration between swarm intelligence and discriminative cluster analysis continues until the satisfactory maximization of FD archives and optimal DMS is discovered [22,23]. Finally, the DMS was used to train a support vector machine (SVM) classifier for distinguishing islets/cells by group membership (pristine or compromised) [24,25]. Full technical details of this analytic strategy, including data augmentation, are described in [13].

2.3. Unsupervised assessment

In the transplantation experiment, where it was investigated whether the DMS could be used to predict restoration of glucose control, a fully unsupervised methodology was applied in order to minimize risk of overfitting. Unsupervised principal component analysis (PCA) [26] was applied to the same multidimensional feature vectors defined by the DMS in order to sort like with like by emergent factors, rather than sorting by known group membership.

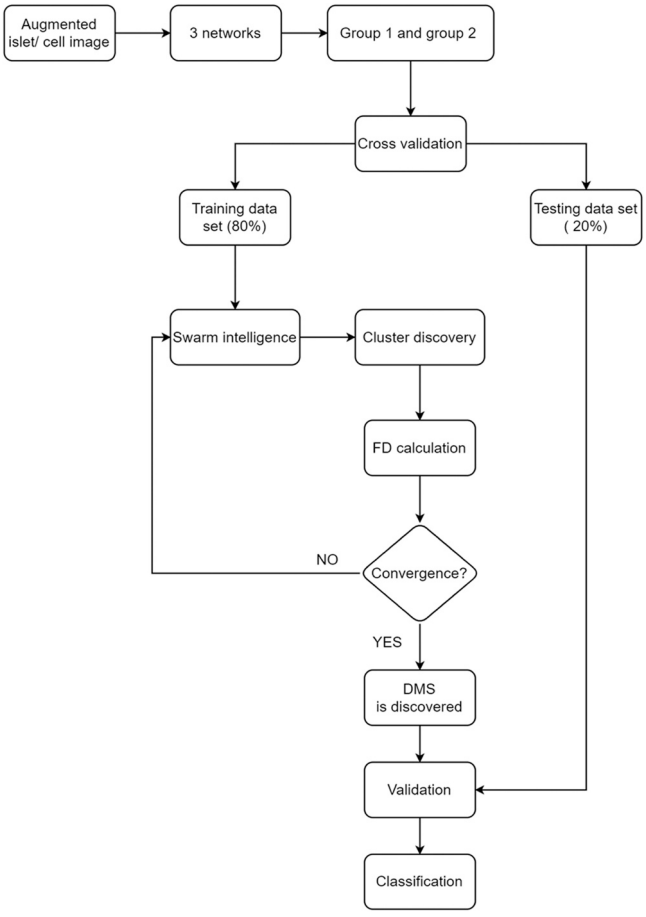

Fig. 1. Data analysis flowchart used in this study.

This approach is known to be suboptimal in constructing an accurate model, but it provides a strong proof of concept as there can be no overfitting. Data was considered at the per islet level as well as the potential for the resultant "viability score" to categorize whole preparations.

3. Results

The application of the DMS was evaluated to differentiate whole islets based on discriminative cluster analysis shown in Fig. 1. The data distribution for each cluster was shown by an ellipse which covers one standard deviation from the median. Cluster separation robustness was measured by quantifying the overlap of the ellipses using intersection over union (IoU) values which vary from 0 % to 100 % for fully separated to fully overlapped. Representative images of pristine, ROS exposed and ischemia exposed islets (Fig. 2). ROS exposure resulted in a clear visible change in islet morphology compared to controls (Fig. 2A and B) – accounting for the very high level discrimination achieved (Fig. 3a) while the impact of ischemia (Fig. 2C) was not perceivable. A brightfield image of an islet with a conformal coating is shown in Fig. 2D.

IoU showed that DMS of whole, single islets (Fig. 3), was successfully able to identify ROS damage (Fig. 3a), inflammatory cytokines (Fig. 3b), DMOG (Fig. 3c) and warm ischemia (Fig. 3d) with IoU found to be 0 %, 3 %, 21 %, 36 %, respectively. When islets were encased in a conformal coating – a procedure which is being advanced for the protection of transplanted islets from assault by the immune system, exposure to pro-inflammatory cytokines was still detectable Fig. 3e) with IoU equal to 21 %. The DMS robustness was successfully validated using the testing data points (further details in Supplementary material, Supplementary Figure 1) put aside during the training process.

To define islet labels a SVM classifier was constructed [19] and trained using associated DMS. Classifier performances were represented in (Fig. 4) by the receiver operating characteristic (ROC) graphs and 95 % confidence interval calculated through bootstrapping methodology [27]. DMS extracted from images of whole, single islets was successfully able to identify ROS damage with 98.8 % accuracy (Fig. 4a), inflammatory cytokines with 88.5 % accuracy (Fig. 4b), DMOG with 76 % accuracy (Fig. 4c) and warm ischemia with 66.8 % accuracy (Fig. 4d). When islets were encased in a conformal coating exposure to pro-inflammatory cytokines was still detectable with 78 % accuracy Fig. 4e).

The same analysis was applied to single cell images from disaggregated islets. For the assessment of single islet cells (Fig. 5) results were mixed, with superior accuracy being obtained for warm ischemia (71 %; Fig. 5D), similar for DMOG (72 %; Fig. 5C), and inferior for inflammatory cytokines (71 %; Fig. 5B) and ROS (80 %; Fig. 5A).

To investigate the translatability of the DMS we transplanted four preparations of control islets and five preparations of islets exposed to warm ischemia to syngeneic diabetic mice. All of the control islet preparations restored glucose control, compared to two of the ischemic preparations. An aliquot of islets were taken from the transplant preparations and imaged. We then analysed these images using an unsupervised methodology of principal component analysis where the algorithm was not "told" which groups to separate, but simply to maximally spread the data based on the islets native characteristics. The principal component analysis was able to separate islets from functional preparations which restored glucose control (Supp Fig. 2) from non-functional preparations which did not, with an ROC AUC of 0.75 (Fig. 5A, C). Importantly, when the median values from the second-highest ranked PCA variable – 'viability score 2′ – were calculated for each preparation (Fig. 6D) a threshold line could be drawn which divided viable from non-viable

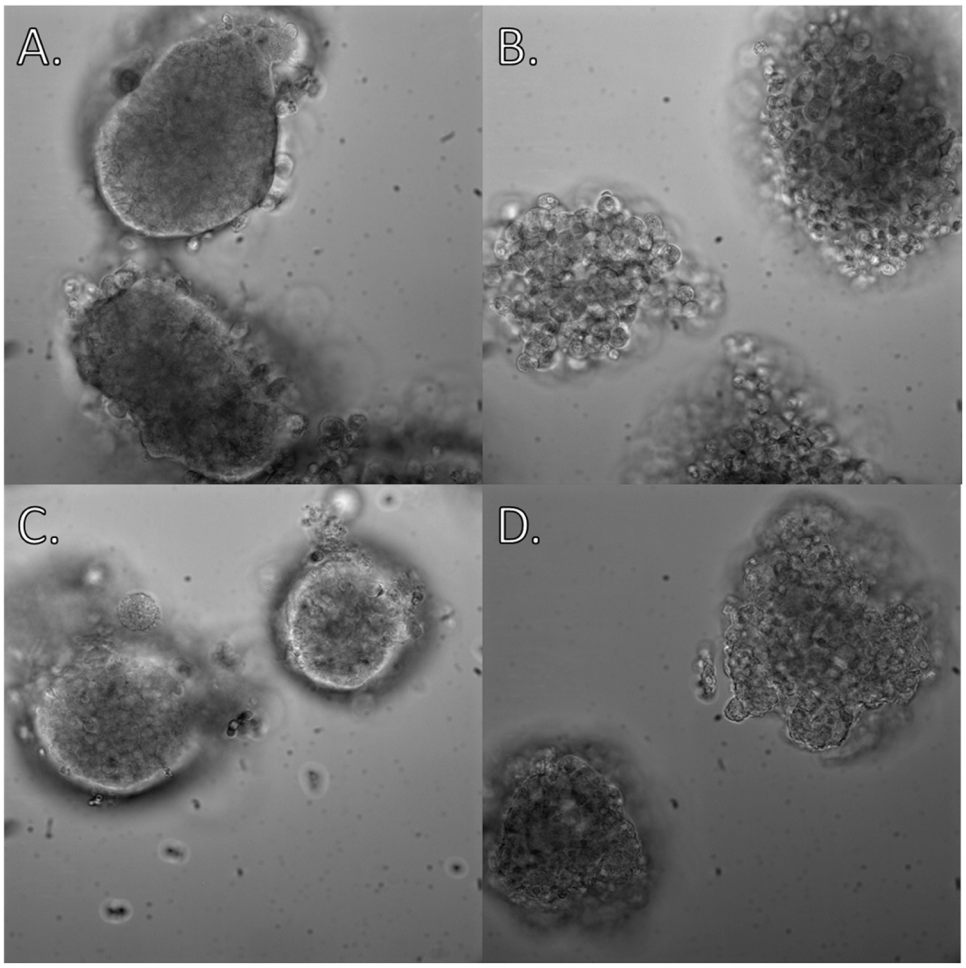

Fig. 2. Brightfield images of islets exposed to A) no insult (pristine); B) ROS treatment; C) Warm ischemia treatment; D) Encapsulation.

preparations. The resulting classification allowed us to accurately predict of transplant success in pristine and ischemic islets.

4. Discussion

The prediction of islet function post-transplantation would be of great utility to inform clinical decision making, however there are no options with sufficient reliability and accuracy for widespread uptake [3–8]. Our DMS enabled individual islets and islet cells to be sensitively categorised according to their exposure to ROS damage, inflammatory cytokine signalling, DMOG and warm ischemia compared to those maintained in pristine resting conditions. The forms of damage that could be most accurately detected varied between whole islets and single cells, with ROS and inflammatory cytokine exposure being most accurately detected in whole islets compared to ROS and DMOG in single cells. Accuracy for both systems was comparable to our success with the hyperspectral assessment of autofluorescence [9].

Changes in islet morphology, detectable to assessors at their most extreme expression, could explain why the forms of damage most clearly detected in whole islets were reduced in single cells, even as accuracy for warm ischemia – the form of damage detected with lowest accuracy in whole islets – was improved for single cells. The interventions most clearly detected (in islets) are likely to be those which produce the greatest damage. These are therefore the interventions which would induce the greatest shift in the macrostructure of the islet which the DMS would only be able to take advantage of in the assessment of whole islets. When the islets were disaggregated to single cells this information was lost – primarily to the disadvantage of the assessment of the interventions where it was most relevant (i.e. those where damage and therefore initial accuracy were highest). However, disaggregation enabled the collection of more data points, which would have been most advantageous in attempts to detect the lightest forms of damage. In those cases (warm ischemia, DMOG) the additional resources for algorithm training may have offset the loss of the macrostructural information. Successful application to single cells additionally shows that this technology could be applied for novel β-cell replacement strategies (e.g. assessing efficiency of stem cell culture and differentiation [28]).

Additionally, we showed that the DMS could be applied to islets treated with a conformal coating with a small loss of accuracy (89 % down to 73 %) in the discrimination of pristine islets from those subjected to inflammatory cytokine treatment. This could be due the conformal coating interfering with the image (for instance, severely damaged islets lose compaction, an effect that is constrained by conformal coating) alternatively, the coating may provide partial protection from the cytokine treatment, reducing the size of the effect for the DMS to detect.

We were additionally successful at using an unsupervised algorithm to classify whether or not an islet preparation would restore glucose control in diabetic mice. Unsupervised analysis provides especially strong 'proof of concept' as it carries no risk of over-fitting due to the analytic methodologies being blind to group membership and instead classifying by emergent differences. Translational work would be better undertaken using more powerful supervised

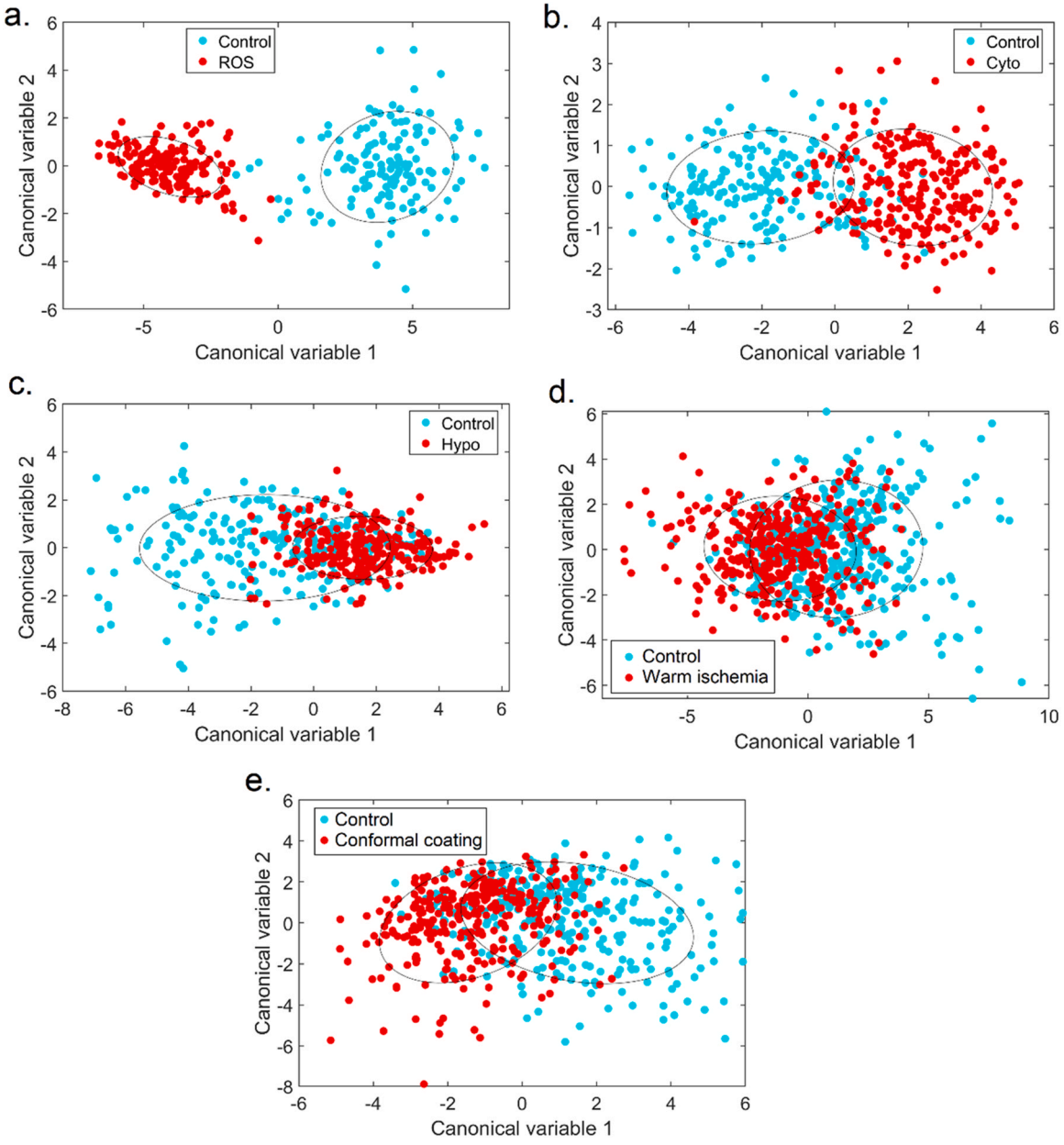

Fig. 3. Cluster separation graphs for whole islet DMS with paired ROC curves for a) ROS AUC= 0.99 Accuracy = 98 %, B) inflammatory cytokines AUC= 0.95, accuracy = 89 %, C) DMOG AUC= 0.83 Accuracy= 76 %, D) warm ischemia AUC= 0.76 Accuracy= 68 %, E) encapsulation AUC= 0.86 Accuracy= 73 %. Individual points on graphs do not represent different cells due to the application of the image augmentation approach to image analysis.

assessment with islets from a larger number of (human) examples to maximise accuracy and reliability, and to investigate the impact of cold ischemia across multiple samples. Further, exposure to cold ischemia, which presents with high potential clinical variability, can be investigated for its impact on the performance of the model. Further work could also involve the impact of exposure to actual hypoxia (1–5 % oxygen) which occurs frequently and for long periods in the clinical environment.

The unsupervised assessment was also able to classify individual islets by whether or not they came from a preparation that would be functional on transplantation. Unlike the classification of whole preparations accuracy was not perfect (Fig. 4C), however, not all islets in a functional preparation will be functional, nor visa versa. These "misclassifications" may therefore indicate the DMS' ability to non-invasively identify functionality at an individual islet level, which could be developed as a tool to enable the study of the cellular basis of transplant failure.

This communication demonstrated the power of computer vision to discover morphological characteristics specific to islet viability that are not noticeable to human visual evaluation of microscopic images. The technique described here does not utilise hand-designed features, which potentially enhances its generalizability because morphology does not require parameterization. The translatability of this approach is reinforced by the fact that it uses basic brightfield microscopy which is widely available. Furthermore, the approach can be non-invasively applied to encapsulated islets – an emerging technology for preventing immune rejection – and single cells from disaggregated islets – a much higher throughput methodology. Finally, it showed sensitivity in distinguishing islet preparations which were capable of restoring glucose control in diabetic mice from those which were not. Future research should involve the collection of brightfield images of human islets being used for transplantation for the treatment of type-1 diabetes, as well as relevant patient (and donor factors) and treatment outcomes. In

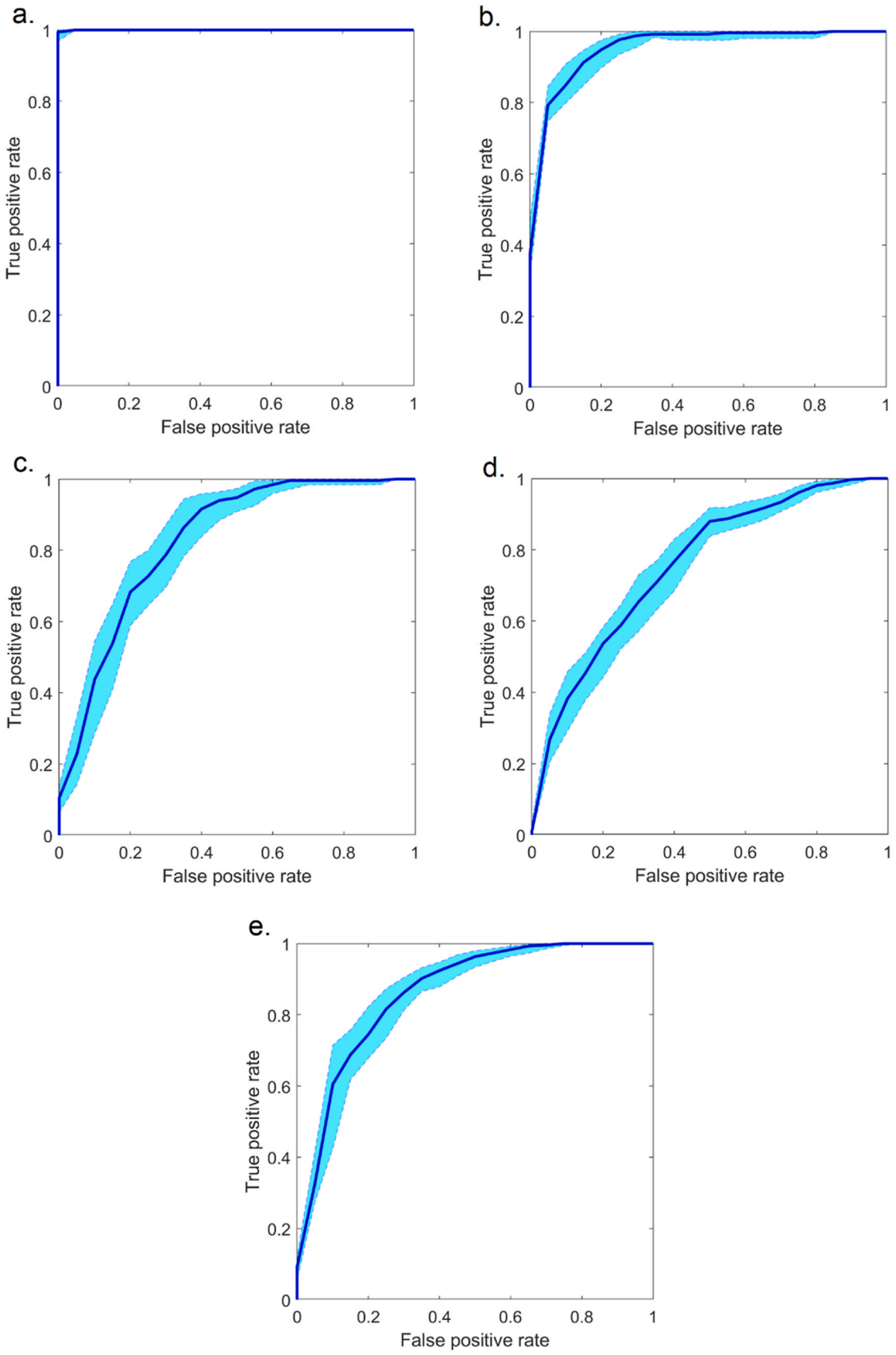

Fig. 4. ROC curve representing DMS classification performance of whole islets. a) ROS AUC= 0.99 ± 0.01 Accuracy = 98.8 %, b) inflammatory cytokines AUC= 0.95 ± 0.01, accuracy = 88.5 %, c) DMOG AUC= 0.82 ± 0.03 Accuracy= 76 %, d) warm ischemia AUC= 0.75 ± 0.02 Accuracy= 66.8 %, E) encapsulation AUC= 0.86 Accuracy= 73 %. Individual points on graphs are non-unique due to the application of the image rotation approach to image analysis.

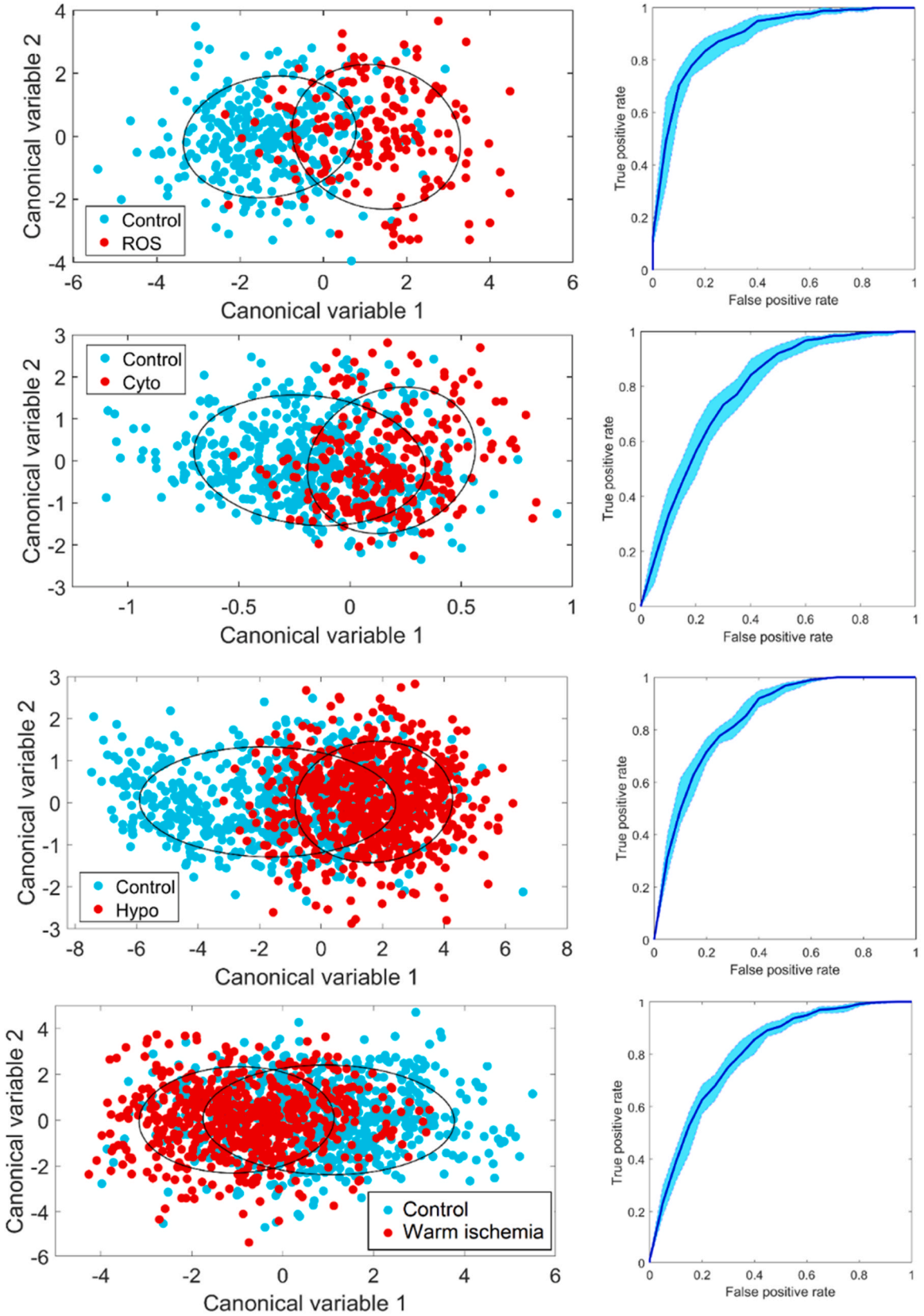

Fig. 5. Cluster separation graphs for single cell DMS with paired ROC curves for a) ROS IoU= 13 %, AUC= 0.89 ± 0.01 Accuracy = 80 %, B) inflammatory cytokines IoU= 30 %, AUC= 0.78 ± 0.03, Accuracy = 71 %, C) IoU= 20 %, DMOG AUC= 0.84 ± 0.01 Accuracy= 72 %, D) warm ischemia IoU= 32 %, AUC= 0.79 ± 0.02 Accuracy= 71 %. Individual points on graphs are non-unique due to the application of the image augmentation (rotation approach) to image analysis.

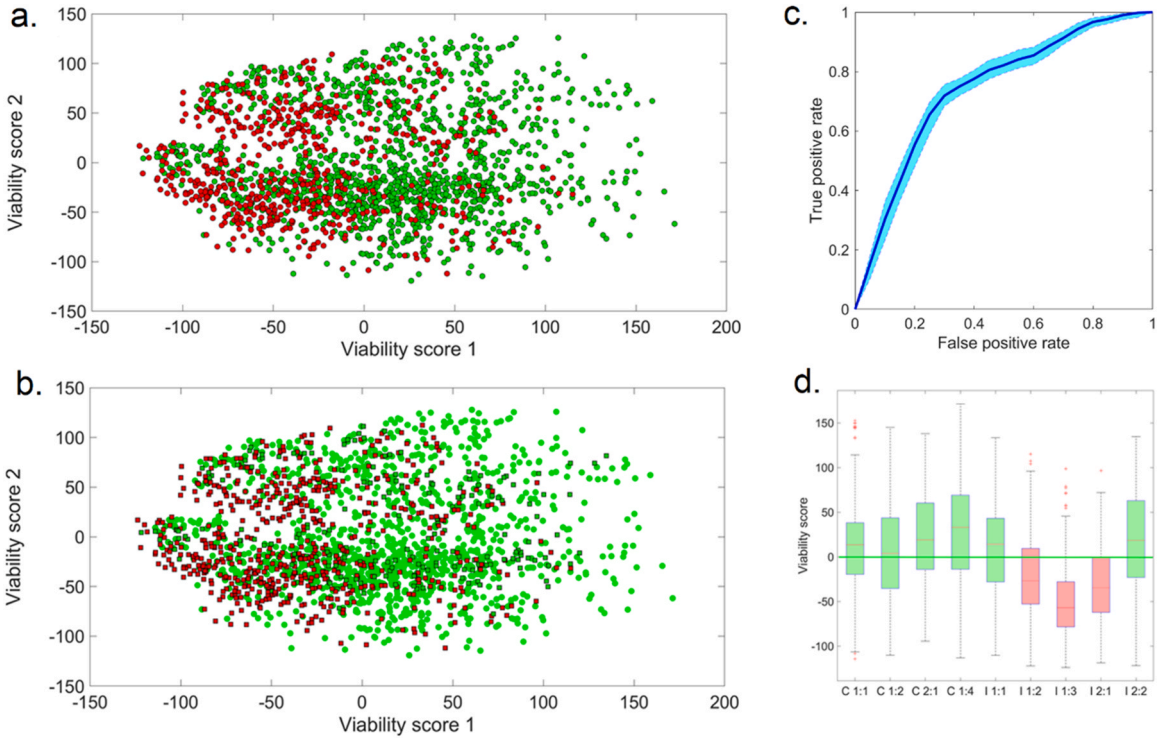

Fig. 6. Unsupervised application of the DMS to transplanted islets. PCA was applied the multidimensional feature vectors of all islets. A) Islets that restored glucose control in transplant recipients (green) plotted against islets that did not (red) in the space spanned by the two PCA components (viability score 1 and viability score 2). B) As previous, but with exposed to ischemia (squares) distinguished from controls (circles) with viability still indicated by green and red. C) ROC curve for the identification of individual islets as coming from viable or non viable preparations AUC = 0.75 ± 0.01. D) Box plots of the values of viability score 2 for the different islet preparations. C = control and I= Ischemia. A threshold\line could be defined that lay below the median value for all viable islet preparations and above the median value for all non-viable preparations. As such, this gave 100 % accuracy for the classification of islets at the group level. Islet preparations labelled as treatment group (C or I), replicate number: preparation number within replicate.

this way a DMS can be trained and tested on human data for eventual clinical translation upon adequate demonstration of accuracy, generalisability and reliability. This would enable the identification of islet preparations with insufficient potential to restore glycaemic function, thereby sparing patients from unsuccessful transplant attempts and significantly reducing patient burden.

CRediT authorship contribution statement

A.H. conceived of this project, performed artificial intelligence, swarm intelligence, discrimination analyses, and biostatistics and prepared the manuscript. JMC SNW, STG and EMG conceived of and contributed to the design of the project, JMC, AGA and SNW participated in data collection, SBM assisted with the statistical analysis, and all authors contributed to interpretation. The manuscript was drafted by JMC and AH with all authors participating in its critical revision. All authors have read and agreed to the published version of the manuscript.

Conflict of Interest

No conflict of interest.

Acknowledgments

A.H is supported by the Cancer Institute NSW, Australia through an Early Career Research Fellowship (ECF1291). This research was also supported by the Juvenile Diabetes Research Foundation (Australia) through the JDRF award 1-INO-2019–788-S-B to S.T.G and E.G. and partially supported by a Discovery Project grant from the Australian Research Council (DP170101863) and the Centre of Excellence scheme (CE140100003) as well as the UNSW SHARP scheme to E.G. The research was also supported by National Health Medical Research Council (NHMRC) grants (GNT1130222; GNT1146493; GNT1189235) and the Twin Towns Services Community Foundation to S.T.G. S.T.G. is a NHMRC Senior Research Fellow (GNT1140691).

Appendix A. Supporting information

Supplementary data associated with this article can be found in the online version at doi:10.1016/j.csbj.2023.02.039.

References

[1] Anazawa T, Okajima H, Masui T, Uemoto S. Current state and future evolution of pancreatic islet transplantation. Ann Gastroenterol Surg 2019;3(1):34–42.
[2] Barton FB, Rickels MR, Alejandro R, et al. Improvement in outcomes of clinical islet transplantation: 1999-2010. Diabetes Care 2012;35(7):1436–45.
[3] Papas KK, Suszynski TM, Colton CK. Islet assessment for transplantation. Curr Opin Organ Transpl 2009;14(6):674–82.
[4] Ricordi C, Lakey JR, Hering BJ. Challenges toward standardization of islet isolation technology. Transpl Proc 2001;33(1–2):1709.
[5] Bertuzzi F, Ricordi C. Prediction of clinical outcome in islet allotransplantation. Diabetes Care 2007;30(2):410–7.
[6] Street CN, Lakey JR, Shapiro AM, et al. Islet graft assessment in the Edmonton Protocol: implications for predicting long-term clinical outcome. Diabetes 2004;53(12):3107–14.
[7] Salgado M, Gonzalez N, Medrano L, et al. Semi-automated assessment of human islet viability predicts transplantation outcomes in a diabetic mouse model. Cell Transpl 2020;29. 963689720919444.
[8] Goto M, Holgersson J, Kumagai-Braesch M, Korsgren O. The ADP/ATP ratio: a novel predictive assay for quality assessment of isolated pancreatic islets. Am J Transpl: J Am Soc Transpl Am Soc Transpl Surg 2006;6(10):2483–7.
[9] Campbell JM, Walters SN, Habibalahi A, et al. Autofluorophores assessed by hyperspectral microscopy indicate perturbation and transplant viability in pancreatic islets. Res Sq 2022. (PrePrint).
[10] Bakal C, Aach J, Church G, Perrimon N. Quantitative morphological signatures define local signaling networks regulating cell morphology. Science 2007;316(5832):1753–6.

[11] Louis CM, Erwin A, Handayani N, Polim AA, Boediono A, Sini I. Review of computer vision application in in vitro fertilization: the application of deep learning-based computer vision technology in the world of IVF. J Assist Reprod Genet 2021:1–13.
[12] Craik A, He Y, Contreras-Vidal JL. Deep learning for electroencephalogram (EEG) classification tasks: a review. J Neural Eng 2019;16(3):031001.
[13] Habibalahi A, Campbell JM, Bertoldo MJ, et al. Unique deep radiomic signature shows NMN treatment reverses morphology of oocytes from aged mice. Biomedicines 2022;10(7).
[14] Walters S, Webster KE, Sutherland A, et al. Increased CD4+Foxp3+ T cells in BAFF-transgenic mice suppress T cell effector responses. J Immunol 2009;182(2):793–801.
[15] Wang J., Perez LJCNNVR. The effectiveness of data augmentation in image classification using deep learning. 2017:11.
[16] Campbell JM, Habibalahi A, Mahbub S, et al. Non-destructive, label free identification of cell cycle phase in cancer cells by multispectral microscopy of autofluorescence. BMC Cancer 2019;19(1):1–11.
[17] Habibalahi A., Campbell J., Mahbub S., et al. moRphology-dEep Learning Imaging Cells (RELIC)-to Differentiate Between Normal and Pathological Kidney Exfoliated Cells. *bioRxiv.* 2022.
[18] Habibalahi A., Moses D., Campbell J., et al. Computed Tomography Radiomics Signatures: Sensitive biomarkers for clinical decision support in pancreatic cancer-a pilot study. *medRxiv.* 2021.
[19] Vapnik V. The Nature of Statistical Learning Theory. Springer science & Business media; 2013.
[20] Tsuda K., Kawanabe M., Müller K.-R. Clustering with the fisher score. Paper presented at: Advances in Neural Information Processing Systems2003.
[21] Habibalahi A, Bala C, Allende A, Anwer AG, Goldys EM. Novel automated non invasive detection of ocular surface squamous neoplasia using multispectral autofluorescence imaging. Ocul Surf 2019;17(3):540–50.
[22] Habibalahi A. Non-invasive cancer characterisation using autofluorescence imaging. Sydney, Australia: Macquarie University; 2019.
[23] Habibalahi A, Moghari MD, Campbell JM, et al. Non-invasive real-time imaging of reactive oxygen species (ROS) using auto-fluorescence multispectral imaging technique: a novel tool for redox biology. Redox Biol 2020;34:101561.
[24] Habibalahi A, Allende A, Michael J, et al. Pterygium and ocular surface squamous neoplasia: optical biopsy using a novel autofluorescence multispectral imaging technique. Cancers 2022;14(6):1591.
[25] Habibalahi A, Allende A, Bala C, Anwer AG, Mukhopadhyay S, Goldys EM. Optimized autofluorescence spectral signature for non-invasive diagnostics of ocular surface squamous neoplasia (OSSN). IEEE Access 2019;7:141343–51.
[26] Maćkiewicz A, Ratajczak W. Principal components analysis (PCA). Comput Geosci 1993;19(3):303–42.
[27] Efron B, Tibshirani RJ. An Introduction to the Bootstrap. CRC press; 1994.
[28] Odorico J, Markmann J, Melton D, et al. Report of the key opinion leaders meeting on stem cell-derived beta cells. Transplantation 2018;102(8):1223–9.